Monitoring, Prediction and Early Warning 20

Kyoji Sassa, Luciano Picarelli and Yin Yueping

Abstract Landslide risk reduction is a societal pressing need in for counties and also areas along coasts, lakes, rivers in relatively flat countries. Engineering measures to stabilize dangerous slopes needs very high cost and not feasible for many cases. Monitoring, Prediction, Early Warning is the most economical landslide risk reduction measure which is applicable for both developed and developing countries. This chapter presents monitoring of triggering factors, slope deformation, other indicators in indoor experiments, field experiments as well as in natural condition. Methodology of prediction and early warning is examined based on these monitoring and topographical, geological and hydrological conditions.

Keywords Early warning • Time prediction • Real time monitoring • Real time warning system • Model experiment • International Programme on Landslides (IPL)

20.1 IPL C105 "Early Warning of Landslides"

Members of International Consortium on Landslides and other related landslide researchers together with representatives from United Nations organizations (UNESCO, WMO, FAO, UN/ISDR, UNEP, UNDP, UNU) and global NGO (World Federation of Engineering Organizations) etc gathered at the opportunity of Round Table Discussion for strengthening research and learning on landslide risk mitigation in Tokyo and promoting the International programme on Landslides in January 2006. Asian members discussed and decided to propose a project focusing currently important topics on landslides in Asian Country. Then, the International Consortium on Landslides applied a budget to the Ministry of Education, Sports, Culture, Science and Technology (MEXT), Japan within an Asian joint Research framework titled as "Asian Joint Project: Early Warning of Landslides" together with Korea, China, Indonesia, Thailand, Philippines and Japan. It was fortunately approved in 2007 as 3 years project (2007–2009).

Figure 20.1 presents the concept of proposed Asian joint project. "Early Warning of Landslides". The development of effective early warning technology needs various factors.

(1) The central flow from top to bottom is from the monitoring of triggering factors (rainfalls, snow

Kyoji Sassa (✉)
International Consortium on Landslides

Luciano Picarelli
Seconda Universtà di Napoli, Italy

Yin Yueping
China Geological Survey, China

K. Sassa, P. Canuti (eds.), *Landslides – Disaster Risk Reduction*,

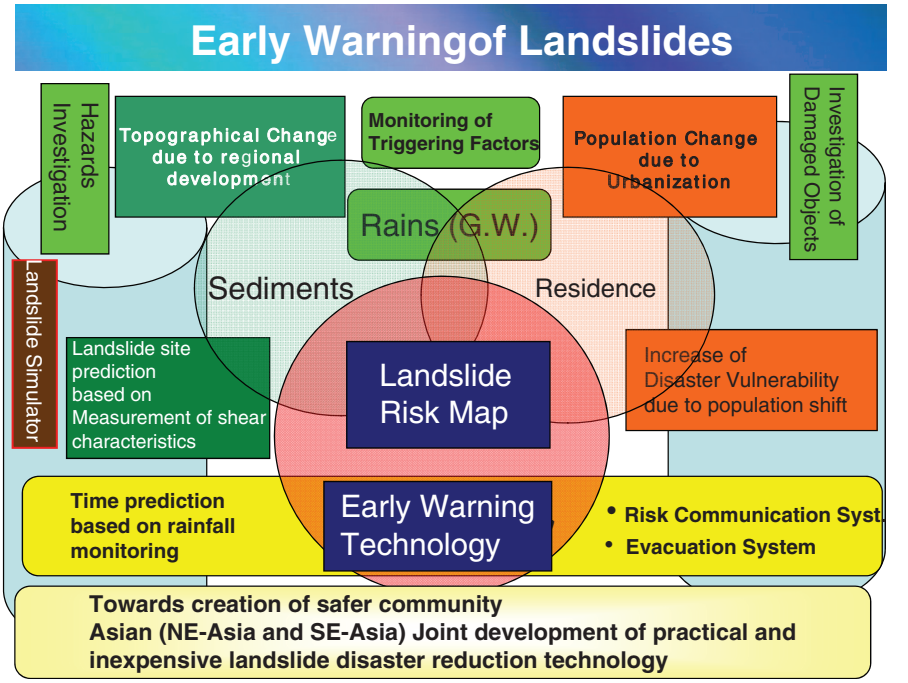

Fig. 20.1 Concept of IPL C105 early warning of landslides

melts, ground water levels) to development of landslide risk map and of early warning technology, then contributing to the creation of safer community.

(2) The left flow from top to bottom represents a aspect of technology for site and time prediction of landslides. Topographical change due to regional development has big impact on landslide risk. Landslide simulator (Dynamic loading undrained ring-shear apparatus (Sassa et al., 2004) to reproduce the formation of sliding surface and post-failure motion within an apparatus (Landslide simulator) is a strong tool for that.

(3) The right flow from top to bottom represents a social aspect. Population change due to urbanization has a great impact on landslide risk. The investigation of exposed objects is important for disaster assessment. Increase of disaster vulnerability due to population shift shall affect landslide risk map. Human or social aspect of Early Warning is risk communication system and evacuation system. Those developments will give great influence on effective early warning to reduce fatalities.

Figure 20.2 presents landslide types concerning landslide risk. Early warning is often issued without

Landslide Types affecting Risk

	Rapid Motion ⟷ Slow Motion	
Deep Slides ⇕ Shallow Slides	(Rapid and Deep) Deep-sheeted rapid landsides	(Slow and Deep) Reactivated landslides
	(Rapid and Shallow) Liquefied failures and debris flows.	(Slow and Shallow) Surface layer creep

- Landslide risk is affected by velocity and depth.
- Risk is different in areas (urban and rural)
- Landslide risk should be evaluated for each type of velocity, depth and area.

Fig. 20.2 Landslide susceptibility mapping and time prediction for early warning

any mention of landslide type. However, Landside risk is quite different by landslide types. Landslides can be classified with regard to depth and speed from the aspect of risk. Deep and rapid landslides are most dangerous as single landslide. Shallow and rapid landslides are also dangerous especially when many landslides will occur during the same triggering event.

Slow landslides are relatively safe for people since they allow evacuation even during motion. However, often villages are constructed on reactivated landslides (previously landslide occurred and relatively flat areas are provided by past landslide events).The velocity is not so high, and travel distance is not great in this type of landslides. However, landslide movement can be enough to destroy houses, schools, and other buildings. The failure of houses and other structures may give damages to humans. Shallow and slow landslides are relatively not dangerous. Often early warning is not specified on these landslide types. Deep and shallow, rapid and slow movements have different mechanism, so the same criteria of early warning cannot be applied. We have to develop some criteria for different types. Risk is very different in urban environment or rural areas.

For reliable landslide risk mapping, the measurement of shear characteristics of soils is the most important. Shear characteristics mobilized during motion of landslides is available from the Landslide Ring-shear Simulator (undrained dynamic-loading ring-shear apparatus, Sassa et al., 2004). For triggering of landslides, pore-water pressure is the most important factor. Therefore, it is better to correlate the initiation of landslides with ground water level than rainfall itself. One possibility is to use a tank Model or leakage barrel model. Some application of tank model to simulate ground water level or volume of ground water for Zentoku landslides and landslide triggered by 2004 Niigata-ken Chuetsu earthquake are reported in Hong et al. (2004), Okada (2004). Some time prediction methods are presented by Picarelli, Versace, Jakob in this chapter.

The Asian joint project group proposed to organize a session on early warning of landslides in the First World Landslide Forum. The Italian group headed by Luciano Picarelli and others joined this initiative. The landslide research community has to cooperate to develop a new economical and effective based on mechanism of landslides, namely early warning technology. The followings are the basic consideration by Picarelli, and contribution from initial participants.

20.2 The Concept of Early Warning

Early warning is the whole of the actions to be taken before a catastrophic event, allowing individuals to take action in order to avoid or reduce the impeding risk (Gasparini et al., 2007). Lead time is the time interval comprised between the moment when the occurrence of the event is reasonably certain, and the moment of its actual occurrence.

In the last years, early warning systems have been employed for protection against some natural risks. In some cases, as for heavy meteorological events, volcanic eruptions and tsunami, they prove quite efficient, since the lead time available to take action, as evacuation or protection of some key structures and infrastructures, is long enough. In other cases (as for earthquakes, flash floods, rapid landslides), the lead time is so short that radical solutions for risk mitigation cannot be undertaken. In these cases, early warning can be adopted only for very limited goals or the signal must be launched well before the expected event, i.e. when its probability is high enough but it is not really certain. This last approach implies subjective decisions and can lead to false or missing alarms.

In case of rapid landslides, since the time elapsing between the onset of slope failure and its impact on exposed goods is typically in the order of tens of seconds, the problem is similar to the one posed by earthquakes, for which advanced procedures are being experienced (Gasparini et al., 2007), but even more complicated because often landslides may occur everywhere within wide areas which lack any type of instrument able to recognize the occurrence of the event. Research in this field is active, even though just beginning.

20.3 Landslide Prediction

The prediction of landslide triggering is a fundamental step in the setting up of early warning

systems. In principle, prediction may be based on the analysis and elaboration of the precursors (rainfall), of indicators of impending rupture (pore pressure changes in the subsoil, ground displacements etc.) or of both.

Based on the collection of data regarding precipitation-induced landslides and triggering rainfall, thresholds have been established in some countries, as Hong Kong (Finlay et al., 1997), California (Wilson & Wieczorek, 1995), New Zealand (Glade et al., 2000) etc. Typically, such thresholds depend on a combination of rainfall intensity and duration; in particular, the critical intensity decreases as the rainfall duration increases. Because of the prominent role of slope morphology, stratigraphy and soil properties, these approaches can be employed only at a local scale. In fact, the relationship between landslide occurrence and rainfall features varies enormously from site to site.

Approaches based on the analysis of indicators of slope failure have been proposed for different types of slope movements. In particular, in the very last years, remote sensing methods are being strongly developed. Unfortunately, these methods can be used only for relatively slow landslides

In the case of rock falls, which occur suddenly, and shortly reach a high velocity, a timely prediction of failure is necessary. Generally, this is pursued through sensors measuring the progressive aperture of rock joints. The analysis of microseismic waves propagating from rock fractures subjected to pre-failure movement is quite a recent approach which is extensively tested in France (Senfaute et al., 2003).

A similar approach based on the analysis and interpretation of pre-failure movements is adopted in the case of creeping slopes (Saito, 1965) and could be used for special conditions, as for slopes subjected to a monotonic pore pressure increase (Picarelli et al., 2004). Failure can be predicted based on an equation fitting displacements recorded during the pre-failure stage, to be extrapolated up to general slope failure. The use of neural networks is another recommended procedure.

Other methods rely on the relationship between pore pressures and ground displacements. Several Authors show that movements of pre-existing slides in clay are activated since the pore pressure reaches a threshold. Through a statistical analysis of collected data regarding a slow mudslide, Mandolini and Urciuoli (1999) propose a relationship between the displacement rate and a combination of the rainfall heights which have been measured in different time spans preceding the present.

Today, a big effort involves researchers involved in the prediction of fast debris flows in unsaturated granular soils. Damiano et al. (2008) discuss a new method to interpret the data provided by TDR devices for a real-time investigation of the changes in the water content profile and consequent suction profile in pyroclastic soils subjected to infiltration. The method, which is being tested by flume tests appears promising, being able to provide reliable information: in fact, it can enable to perform timely analyses of the changes in the safety factor. The same experiences provide further useful data about the use of optical fibres to capture pre-failure soil movements caused by the volumetric collapse which is induced by saturation, and predict the consequent slope failure.

20.4 Implementation of Early Warning Systems

Early warning systems for rainfall-induced landslides are adopted in some regions of the world. In 1977 the Hong Kong Geotechnical Engineering Office established a warning system, which has been continuously updated and improved in the following years (Chan et al., 2003). Similar systems have been used to prevent the consequences of rainfall-induced debris-flows in the S. Francisco Bay (Keefer et al., 1987), in Nagasaki and in other parts of the world. D'Orsi et al. (1997) describe the Rio-Watch, an alert system based on a network of 30 telemetered rainfall gauges and weather radars which cover the city of Rio de Janeiro. Similar systems have been set up in the State of Oregon (Mills, 2002), in UK (Cole & Davis, 2002) and in the area between Seattle and Everett, Washington (Baum et al., 2005). In some countries, some organizations in charge of land protection provide continuous information through the WEB

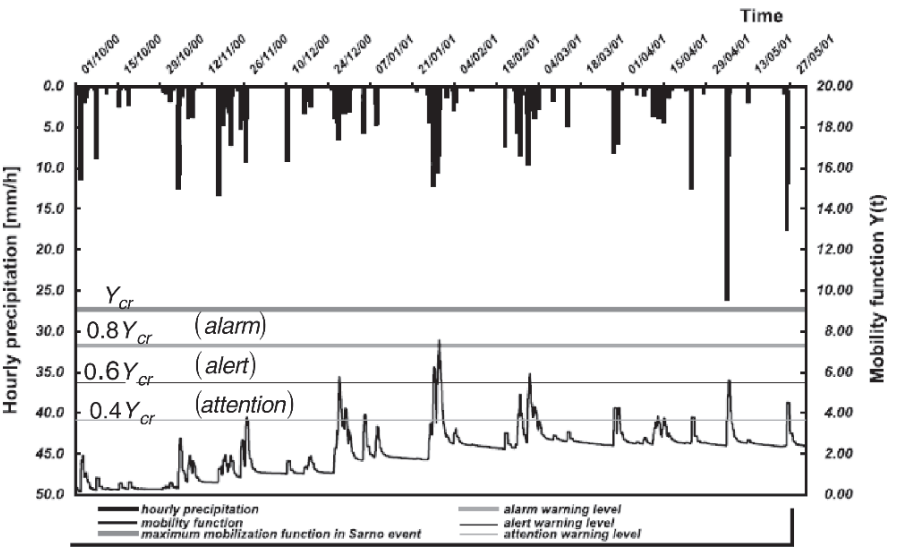

Fig. 20.3 Precipitations and warnings in Sarno area in the period October, 2000, May, 2001 (Picarelli et al., 2008)

about slope stability conditions in critical areas (Flentje et al., 2005).

After the catastrophic events occurred in 1998, an early warning systems has been established in the Sarno area, based on the so called FLAiR model (Forecasting of Landslides Induced by Rainfall), proposed in 1992 by Sirangelo and Versace (Picarelli et al., 2008).

FLaIR consists of two modules: RL (Rainfall-Landslide) and RF (Rainfall Forecasting). Through a calibration of available data collected in the past, the first module correlates precipitations and landslide occurrence in order to determine a mobility function Y(t) which, at any time, depends on the amount of infiltrated water and provides the probability, $P[E_t]$, of landslide occurrence at the time t. The second module provides a probabilistic prediction of impeding rainfall events through a stochastic rainfall or meteorological rainfall nowcasting, which is used to identify hazard conditions for landslide occurrence suitably in advance. Using both modules, the model enables a probabilistic evaluation of potential landslide occurrence.

The adopted strategy for risk mitigation is based on three warning levels: "attention", with instrumental real-time monitoring and real time simulation model running; "alert", involving civil protection agencies and field direct control; "alarm", involving population to be evacuated. A characteristic mobility ratio $\chi = Y/Y_{cr}$, is defined, Y_{cr} being the value of the mobility function associated with each warning level. The choice of the values of the index χ for each warning level must fit considering the necessity to have an adequate safety margin, which needs a low mobility ratio, and to avoid false alarms, which needs a high mobility ratio. Values of the mobility ratio presently used in Sarno are the following: $\chi = 0.40$, for the "attention" threshold, $\chi = 0.65$ for the "alert" threshold and $\chi = 0.85$ for the "alarm" threshold. The average time elapsing between the "alert" and "alarm" signal has been assessed to be in the range 4–5 h, which is considered long enough to assure evacuation.

In Fig. 20.3 are summarised the data on precipitations concerning the wet seasons 2000–2001. It is shown that in the period October, 2000 – June 2001, the attention level has been attained several times, the alert level has been reached three times, while the signal of warning has been launched only one time.

20.5 The Near Future

As shown, hydrological models can be very useful to predict rainfall-induced landslides in well known geomorphological contexts for which documented

data are available. In some cases, as for failure in rock masses and in general everywhere a landslide is expected to occur suddenly and to develop rapidly, the analysis and use of indicators seems a useful criterion. However, rational and advanced approaches should be based on analyses having the goal to simulate the water infiltration and its consequences on the stability of slopes. In fact, numerical analysis could apply in areas occupied by uniform geomaterials whose properties have been adequately investigated in advance. This encourages the use of simplified codes, supported by GIS, as TRIGRS (Baum et al., 2002) which integrate data on rainfall with analysis of infiltration and slope stability over vast areas. A similar approach can be adopted at the scale of the single slope, using well known commercial or purposely develop codes. Today some research programs which follow a strategy based on a real-time use of short-term weather forecasting for slope stability analysis in large areas are active.

However, the still inadequate quality of rainfall forecasting at the scale of single slopes is a prominent problem. Presently, this does not yet allow a confident use of early warning procedures, due to the high probability of false or missing alarms. As a consequence, the numerical analysis should be supported by real-time monitoring of local rainfall and of fundamental indicators, as pore pressure or suction. Since accurate analysis is strongly affected by the difficulty in fixing reliable initial conditions, especially for unsaturated soil (suction), the main advantage of such an approach is that monitoring can provide local values of the pore pressure (or suction), i.e. of the initial conditions (Picarelli et al., 2008). As with FLaIR, the prediction can be carried out using as input a meteorological or stochastic forecasting or rainfall, or a Bayesian combination of both. Therefore, any numerical simulation can start from a correct initialisation of the governing factors. In addition, the continuous check of these factors can lead to a continuous real-time calibration and consequent adaptation of the model.

Just to summarise such considerations, the procedure to be adopted in instrumented sloping areas should require the following steps:

1. rainfall monitoring and forecasting;
2. start of analysis and models routing;
3. model calibration and adaptation;
4. iteration of analysis and prediction;
5. decision making.

In this framework, the basic situation corresponds to "normal" weather conditions, which are characterised by absence of rainfall or by "normal" rainfall. An advisory signal should be launched when weather forecasting anticipates the approaching of an abnormal rainstorm or when the rain gauge network reports unexpected severe rainfall. In case of further warning signals pre-established actions should be activated. A prominent action is strengthening of the monitoring in the instrumented sites and analysis of the likely effects of approaching rainfall (which can be roughly estimated through weather forecasting) accounting for monitored values of pore pressure (or suction): hence, numerical modelling starts to run. Data coming from monitoring should enable a continuous and timely check of the analysis by comparison of calculated and monitored values of pore pressure or suction during rainfall. In fact, the data provided by site monitoring of rainfall and suction can be used to update the initial and boundary conditions as well as other parameters which govern the slope behaviour: hence, the variation of the safety factor of the slope can be continuously adjusted. As a consequence, a framework about what can happen in next hours, i.e. of the presumed scenario of event, should be drawn in the assumption that rainfall will continue with the same intensity, or through stochastic forecasting of continuing rainfall. The process should be iterated until possible activation or deactivation of one of the established levels of warning. Decision making depends on the values of the thresholds which have been established. In this phase, any indicator of approaching failure is highly beneficial, supporting next decision.

The problem of early warning is crucial and delicate. In fact, false or missing alarms can compromise its reliability. However, it will certainly become a prominent tool for risk mitigation in the near future, especially in those densely inhabited areas where the hazard of landslides is critical and the social and economical cost of different procedures for risk mitigation too high for the involved communities.

20.6 Empirical Hydrological Models for Early Warning of Landslides Induced by Rainfall

Pasquale Versace (Università della Calabria, Italy)

The risk of landslide is extremely variable. In fact, slope movements have a wide range of velocity, size and run-out, thus their magnitude and impact on exposed goods can be either very low or very high, depending on site conditions, material involved and other factors. Velocity not only affects landslide destructiveness, but also the procedures to adopt for risk mitigation. Velocity can range between some tens of metres per second (as for rock falls and avalanches, debris flows and flowslides) and some millimetres per year (as for active slides in clay and some lateral spreads).

Early warning can be defined as the entirety of actions to be taken during the lead time, that is, the time interval elapsed between the moment of precursor occurrence and the moment of its actual occurrence. In more general terms, early warning is the provision of timely and effective information allowing individuals exposed to hazard to take action in order to avoid or reduce the damage and the loss of life.

From a general point of view, there are four crucial moments in landslide early warning, such as: precursor forecasting, precursor occurrence, event initiation and impact on people and goods (Picarelli et al., 2007).

Early warning systems prove quite efficient when the time between the detection of first reliable precursors and initiation of the event or between the initiation of the event and the impact on exposed goods is sufficiently long to take action such as evacuation or protection of structures and infrastructures.

When the time between the event and its impact is extremely short, adoption of early warning procedures must be based on precursor measurements. This is the case of rapid landslides, as the time elapsing between the onset of slope failure and its impact on exposed goods is typically in the order of tens of seconds.

When the time between precursor occurrence and event initiation is also short the forecasting of the precursor becomes indispensable. This is the case of shallow landslides when the time between the precursor and the event is in the order of tens of minutes.

Rainfall is largely adopted as a precursor for early warning of landslides, owing to the large prevalence of landslides induced by rainfalls.

The identification of the precursor is the most important issue in landslide forecasting, so the relationship between landslide triggering and intensity or duration of rainfall has been largely investigated to identify threshold values.

Based on the collection of data on landslides and related triggering rainfall, thresholds, often based on a combination of rainfall intensity and duration, have been obtained for several regions, as Hong Kong (Finlay et al., 1997), California (Campbell, 1975; Wilson & Wieczorek, 1995), New Zealand (Glade et al., 2000) etc.

In some of these countries, early warning systems have been conceived to prevent disasters. In fact, these thresholds, in combination with rainfall forecasting and real-time rainfall monitoring, can lead to operational landslide warning systems. As an example, in 1977, the Hong Kong Geotechnical Engineering Office established a Landslip Warning System, which has been continuously updated and improved over the years (Chan et al., 2003). Similar systems have been elaborated to prevent the consequences of rainfall-induced debris-flows in the S. Francisco Bay (Keefer et al., 1987) and in Nagasaki (Yano & Senoo, 1985). D'Orsi et al. (1997) report the Rio-Watch, an alert system based on a network of 30 telemetered rainfall gauges and weather radars covering the city of Rio de Janeiro, which issued 42 warnings between 1998 and 2003. Similar systems have been set up in the State of Oregon (Mills, 2002), in the UK (Cole & Davis, 2002) and in the area between Seattle and Everett, Washington (Baum et al., 2005). Even though a true early warning system has not been set up, in the landslide prone area around Wollongong, Australia, a monitoring system is active and provides continuous information through the WEB with regard to the slope stability conditions (Flentje et al., 2005).

Previous considerations show that today prediction of rainfall-induced landslides is mostly carried out through the so-called hydrological models (Fukuoka, 1980; Mitchue, 1985; Cascini & Versace, 1988), which are based on historical data regarding

landslides and related triggering rainfall and do not require field instrumentations and measurements. *Hydrological* models are distinct from *physically-based* models, which attempt to reproduce the physical behaviour of the processes involved at hillslope scale. These models are complex and need many field investigations and surveys.

In Italy, Sirangelo and Versace (1992) proposed the general hydrological model FLaIR (*F*orecasting of *L*andslides *I*nduced by *R*ainfall), which has been recently extended to mudflows, in pyroclastic soils, occurred in Sarno area on May 1998 (Versace et al., 1998, 2003, 2007).

FLaIR consists of two modules: the *R-L module* (*R*ainfall–*L*andslide) correlates precipitation and landslide occurrence, in order to determine a *mobility function* $Y(t)$, which, at any time, depends on the amount of infiltrated water. This module enables model calibration and permits the reproduction of historical movements (Fig. 20.4).

The second module, *RF* (*R*ainfall *F*orecasting), provides a probabilistic evaluation of rainfall events through a stochastic modelling or meteorological nowcasting. It is used to identify hazard conditions for landslide occurrence suitably in advance.

Using both modules, the model enables a probabilistic evaluation of future landslide occurrence.

In the RL module the mobility function $Y(t)$ is associated with the probability $P[E_t]$ of landslide occurrence at the time t, by the relation:

$$P[E_t] = g[Y(t)] \tag{20.1}$$

where $0 \leq g(.) \leq 1$.

Among various relationships a simple threshold scheme can be assumed: the event is certain if the mobility function $Y(t)$ exceeds the threshold value Y_{cr} and impossible if this value is not exceeded. The mobility function can be linked to the antecedent rainfall $P(.)$ through the expression:

$$Y(t) = \int_0^t \psi(t-u)P(u)du \tag{20.2}$$

where $\psi(.)$ is a filter function which plays a critical role, because the choice of this function can model a wide range of situations.

The value $Y_\tau(t)$ that the mobility function will assume at time t, calculated at the time $\tau(\tau < t)$, may be written splitting the convolution integral (2) into two parts:

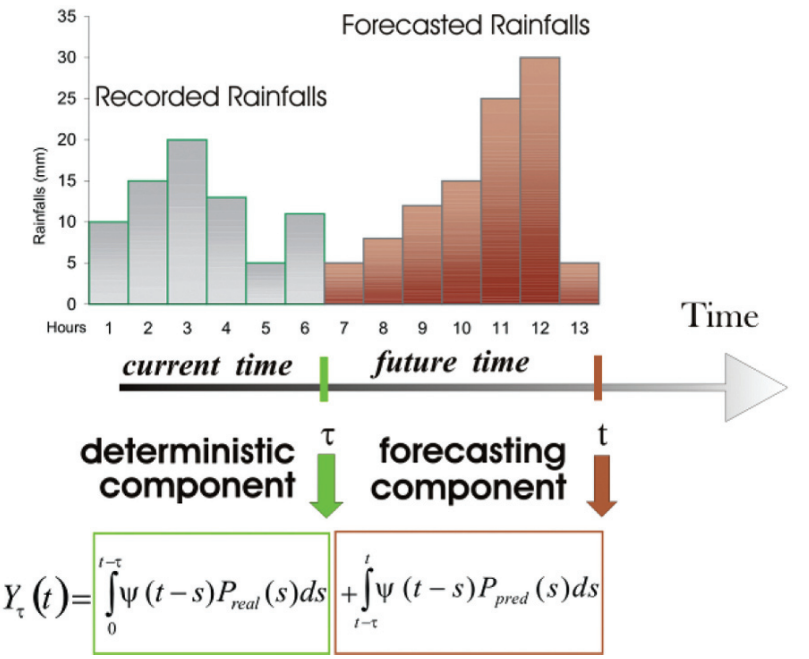

Fig. 20.4 Synthetic scheme of the mobility function components

$$Y_\tau(t) = \int_0^{t-\tau} \psi(t-u) P_{real}(u) du + \int_{t-\tau}^{t} \psi(t-u) P_{pred}(u) du \quad (20.3)$$

the first one, on the right-hand side, can be considered as the deterministic component and is calculated on the basis of observed rainfall P_{real} recorded rainfall up to time τ.

The second one is the stochastic component, associated to the predicted rainfalls P_{pred} which should fall in the interval $[\tau, t]$ and that can be estimated through rainfall forecasting models.

As a consequence, the model may be usefully employed to forecast the hazard of rapid landslides induced by rainfall, allowing the activation of the necessary procedures for civil protection.

The strategy of the civil protection agency with respect to landslide events is usually based on three warning levels: "attention" (or "advice"), with instrumental real-time monitoring and real time simulation model running; "alert" (or "watch"), involving civil protection agencies and field direct control; "alarm" (or "warning"), involving population to be evacuated. Using FLaIR, a characteristic mobility function ratio $\chi = Y/Y_{cr}$ can be associated with each warning level (Fig. 20.5).

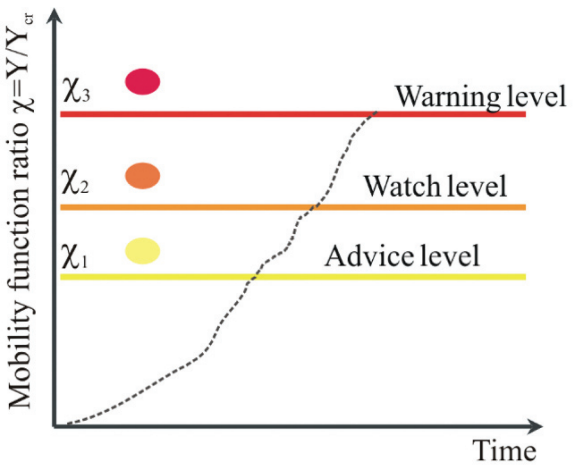

Fig. 20.5 Real time control of the mobility function ratio for evaluating the different critical situations

20.7 Landslide Monitoring, Prediction and Early Warning in Banjarnegara, Indonesia

Teuku Faisal Fathani, Dwikorita Karnawati (Gadjah Mada University, Indonesia), Kyoji Sassa (ICL), Hiroshi Fukuoka (Kyoto University, Japan), Kiyoshi Honda (Asian Institute of Technology, Thailand)

Abstract Landslide is one of most major disasters in Indonesia due to the susceptibility of the region and socio-economical conditions of the country. Since 2007, a community-based early warning system has been introduced in a pilot area at Banjarnegara, Indonesia. Simple extensometers and automatic raingauge have been installed for landslide monitoring and prediction with the participation of local community. Furthermore the Asian Joint Research Project for Early Warning of Landslides consisting of International Consortium of Landslide (ICL), Gadjah Mada University (GMU), Disaster Prevention Research Institute of Kyoto University (DPRI/KU) and Asian Institute of Technology (AIT) have conducted a preliminary investigation and established a real-time monitoring and early warning system at that pilot area. The outdoor unit of fieldserver gathers the data from multiple sensors (two long-span extensometers, raingauge, IP camera and water pressure sensor), whereas indoor processing unit will store data on the monitor, and send the data to AIT server through GPRS modem to be displayed in a webserver.

20.7.1 *Background of Landslide Early Warning in Indonesia*

As the dynamic volcanic-archipelagoes, more than 60% of Indonesian region are covered by the mountainous and hilly areas of weathered volcanic rocks, which are intersected by faults and rock joints. These geological conditions give rise to the high landslide susceptibility of the region. Moreover, the high rain precipitation which can exceed 2000–3000 mm per year, frequent earthquake vibrations as well as the extensive landuse changing and deforestation cause the occurrence of

landslides frequently increase recently. Since the last 7 years, more than 36 landslide disasters occurred and result in 1226 people died or missing. Urgently, some efforts should be done to avoid or reduce the risk of landslides. Unfortunately, most landslide susceptible areas have very fertile soils and very good quality and quantity of water. This makes the susceptible areas are densely populated, and it create serious inducement to slope instability. Despite an effort to establish slope protection zone, which is restricted for any development and settlement, the relocation program is not easy to be carried out due to socio-economical constrains. Therefore, landslide monitoring, prediction and early warning system are urgently required to guarantee the safety of community living in such area.

20.7.2 Geological Condition of the Study Area

A pilot area for landslide monitoring, prediction and early warning program has been established in Banjarnegara Regency, Central Java Province, since year 2007. Based on the site investigation, it is clarified that not only the rain intensity but also the morphology and geological conditions of study area significantly control the occurrence of landslides. The unstable zone in the study area is situated at lower slope of mountains with the slope inclination of 20–60° (Fig. 20.6). The moving materials consist of colluvial deposits of silty clay overlying the inclined impermeable layer of clay, which is situated at the lower part of the andesitic breccias mountain. The clay layers are inclined at the same direction of the slope (i.e. 85°) and this becomes the sliding failure for the above colluvial soils. The moving zone is saturated at most of the rainy season due to the lower position of the zone comparing to the surrounding mountainous slopes. The existence of impermeable clay layer underneath the colluvial soils creates the saturation condition within colluvial soil gradually increased and maintained during the rainy season, until then the rise of pore water pressure within this soil induces the movement. Therefore, monitoring of the pore water pressure (groundwater table) in response to the rain infiltration should be the main concern in establishing early warning for the slope movement.

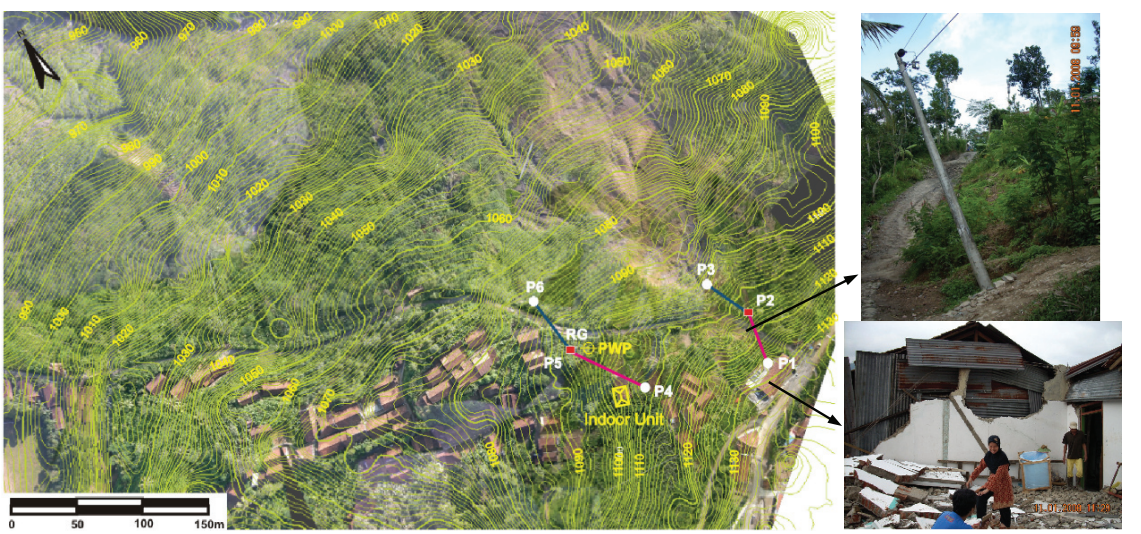

Fig. 20.6 Aerial photo, topography map and position of real-time monitoring equipment. Landslide fatalities are shown on the right

20.7.3 Community-Based Early Warning System

At the beginning of year 2007, Gadjah Mada University has developed simple and low-cost equipment for landslide monitoring and early warning, where the local community in remote areas can easily operate and maintain the equipment based on their own capability. As the initiation of quantitative investigation, two types of simple extensometers and automatic raingauge were installed at a pilot area in Banjarnegara. The first type of extensometer is a handmade manual reading extensometer. Another type is the automatic extensometer, where the relative movement between two points is mechanically enlarged by 5 times and recorded on a paper continually. Both types of extensometers are connected to the siren system in order to directly warn the local community for taking necessary actions in dealing with landslide disaster. Furthermore, a simple modified raingauge has also developed with hourly rainfall intensity recorded on a paper continually. This raingauge is also connected to the siren system to warn the community if the precipitation reaches a certain value. During the installment, five local operators have been trained on how to install and operate this simple equipment (Fathani & Karnawati, 2007).

20.7.4 Real-Time Monitoring and Early Warning System

In line with the installation of simple monitoring equipment, on September 2007, the Asian Joint Research Project for Early Warning of Landslides has conducted a field survey to support the installation of real-time landslide monitoring equipment. This system presents the results of real-time measurement by using long span extensometers, raingauge, pore pressure sensor, and monitoring scene by IP camera. The real-time monitoring equipment consists of outdoor unit and indoor unit. Outdoor unit is fixed on a center pole consists of fieldserver, two extensometers, raingauge, IP camera and water pressure sensor (Fig. 20.7). Fieldserver is a sensing device with real-time online data display system which gathers the data from multiple sensors and shows them in a webserver. The extensometer placed at two positions connected by a pulley and a super invar wire which can measure both extension (+) and compression (–). Indoor unit has two crucial components i.e. processing unit and GPRS modem. Indoor unit collects the data, then process and store data on the monitor, and send the data to AIT server every one hour. This unit also implements early warning that can be adjusted depending on the site condition.

Figure 20.6 shows the aerial photo and topography map of the landslide area mapped by the Balloon Photogrammetry System. This system combines the balloon aerial photography and digital photogrammetry for low-altitude aerial mapping. The balloon carries out a digital camera up to 400 m above the ground level and takes aerial photographs in appropriate viewing angle. The digital photogrammetry processes the photo-restitution to produce 3D model from the multi-view aerial photograph (Rokhmana, 2007).

The position of long-span extensometers poles (P1 to P6), raingauge, pore water pressure sensor and indoor unit are shown in Figs. 20.6 and 20.7. The installation of three poles (P1 to P3) were conducted on December 15th, 2007. The installation process had faced some problems since the slide occurring also on day of the system set up. As shown in Fig. 20.8, starting from December 23rd, 2007, the extensometer has been saturated (up to 660–920 mm of displacement), therefore it cannot measure the movement when the landslide occurred on December 30th, 2007, which destroyed the center pole (P2), buried the lowest pole (P3) and also attacked several existing houses, farm land and district road.

On January 19th, 2008, the monitoring system has been reinstalled at a new location about 150 m from the previous destroyed place (Fig. 20.6). Three new poles (P4 to P6) were erected with two long-span extensometers, raingauge and IP camera connected to center pole (P5). Pore water pressure sensor is placed inside a well near P5, whereas the indoor unit located in a house belongs to a volunteer resident near P4. The result of measurement of two extensometers, daily

Fig. 20.7 Outdoor unit of real-time monitoring equipment

rainfall and pore water pressure fluctuation are shown in Fig. 20.8 The accumulated movement of extensometer starting from January 19th until May 31st 2008 reaches of about 30 and 220 for Extensometer P4–P5 and P5–P6, respectively. Meanwhile the maximum rate of rainfall could reach 200–360 mm/day. It can be seen that the extensometer movements on March 7th and April 13th, 2008 were strongly related to the rainfall occurrence.

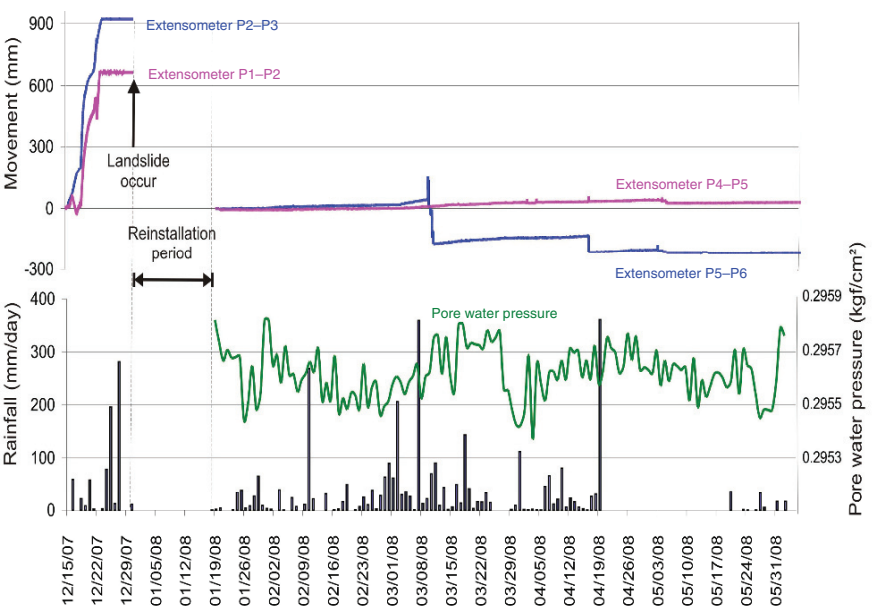

Fig. 20.8 The results of measurement by extensometers, raingauge and pore water pressure sensor

20.7.5 Conclusions

Some lesson learned can be derived from this program that the warning system should be based on a real-time telemetric system with the involvement of community participation. Therefore, both technical skill and communication skill are the main requirements to achieve the success of early warning system program. The system should include some technical aspect such as the geological surveys and site selection, development of equipment design which is simple (low cost) but effective, determination of early warning levels, installment and operation/maintenance at the field site, as well as include the social aspect such as social mapping and evaluation, public consultation and dissemination of program, community empowerment (including the technical training and evacuation drill) for landslide hazard preparedness and operational system of the early warning. Moreover, the communication with all stake-holders such as local, regional and national authorities, local leaders, local youth communities, and local non government organization should be established and maintained. The role of scientist or researcher is more like to be the motivator and facilitator, instead of the instructor or manager of program.

20.8 Early Warning of Landslides Based on Landslide Indoor Experiments

Katsumi Hattori, Hitomi Kohno, Yasunari Tojo (Graduate School of Science, Chiba University, Japan), Tomomi Terajima (Disaster Prevention Research Institute, Kyoto University, Japan), Hirotaka Ochiai (Forestry Agency of Japan)

Abstract An experiment to induce a fluidized landslide by artificial rainfall has been conducted on an indoor slope. The experimental slope is 10 m long, 1 m wide, and the slope gradients are 10° for the lower and 32° for the upper slope. A landslide initiated 65440 s (1h49m40 s) after the start of sprinkling at a precipitation intensity of 80 mm/h. During this experiment, pore pressure, self-potential, and soil displacement have been measured. The results suggest the relationship among motion of subsurface water, soil displacement, and electrical potential differences. Self-potential method seems to have capability for early warning system for landslides.

20.8.1 Introduction

Rainfall-induced landslides often cause catastrophic disasters. In order to mitigate the disasters, monitoring and forecasting of the landslides are important. There are hydraulic and geotechnical knowledge prior to a landslide based on the indoor and outdoor experiments (Ochiai et al., 2004). They are based on pore pressure and soil displacement using gaugemeters and CCD video cameras, respectively. The obtained facts are as follows; (1) development of the saturated area under the surface, (2) direction of the filtration of water changes from vertical to lateral to the slope, and (3) beginning of the apparent soil displacement about a few tens minutes before the catastrophic slide. On the other hand, the geophysical exploration method is one of powerful tools for subsurface monitoring such as electrical resistivity. The electrical resistivity tomography approach shows the slip surface very precisely and continuous measurements of resistivity could be helpful to identify the water condition under subsurface (Perrone et al., 2004) (Lapenna et al., 2005). Self-potential method is also applicable to monitor underground fluid motion based on the electro kinetic effect (Ishido & Mizutani, 1981). Laboratory experiments and geothermal application show the high capability to detect subsurface water motion (Rizzo et al., 2004), (Sasai, 2008), (Zlotnicki & Nishida, 2003). Self-potential method is passive measurement and simple in comparison with electrical resistivity tomography. In this paper, self-potential approach is conducted to develop an early warning system for landslides. The results of a laboratory experiment under precipitation control show the capability to monitor the underground water condition using self-potential method.

20.8.2 The Laboratory Experiment

The laboratory experiment of landslide under the precipitation control has been carried out to

investigate electrical properties and understand the physical process associated with landslides. The background of this experiment is as follows. Based on the previous hydraulic knowledge, (1) the rain water penetrates vertically at the initial stage because of the unsaturated condition. (2) As a saturated area is developed, the water flow pattern turns to the lateral to the slope. (3) From geotechnical point of view, significant soil displacement starts about a few tens minutes before the main collapse. Then, a landslide takes place. The purpose of the experiment is to investigate whether electrical potential changes show those of hydraulic and geotechnical conditions.

The overview of the laboratory experiment system is shown in Fig. 20.9. The angle of an upper slope was 32° and that of a lower slope was 10°. The length and width of a slope are 9 m and 1 m, respectively. The soil density in the slope was almost uniform and the thickness was 70 cm. The soil is weathered granite and averaged grain radius is 0.39 mm. There is a sprinkler for an artificial precipitation. The intensity of the precipitation was controlled by 80 mm/h. 40 mm rain (with 80 mm/h) was precipitated two days before the experiment. It was found that water came out of from the slope very slowly. It means that groundwater system has been created before the experiment. It seems rather natural situation. A rubber sheet is used for insulation.

Pore pressure, self-potential, and soil displacement measurements have been performed. As for self-potential measurements, electrodes (Pb-$PbCl_2$), pasted the bentonite to reduce a contact resistivity, have been installed with intersensor distance of one meter in a depth of 20 cm and 50 cm and the reference electrode has been installed in the depth of 50 cm at the top of the slope. For pore pressure measurements, gauge meters have been set up in a depth 10 cm, 40 cm and 65 cm with one meter spacing. Here, electrodes and pore pressure meters were installed alternately. The electrodes and gauge meters have been connected to the 16 bit AD converter (National Instrument SCXI-1120) and fed to the data acquisition PC. The sampling rate is 100 Hz. Soil displacement has been recorded by CCD video cameras with motion of markers. The total amount of water flowed out from the slope has also been measured.

The landslide occurred at the upper slope 65440 s (about 110 min) later from the beginning of the precipitation. Thus, the total amount of the rain fall was about 145 mm.

Fig. 20.9 Indoor experiment system of an artificial slope under precipitation control

20.8.3 Observed Data

Figure 20.10(a,b) illustrate the 2D variation of hydraulic and electrical properties, respectively. The sequence of figure corresponds to the time progress after the precipitation start. The time stamp is given beside the panel. In Fig. 20.10(a), the color and contour indicate the pore pressure and hydraulic head. In Fig. 20.10(b), the color and contour show the potential differences the electric field. From Fig. 20.10(a), we found that filtration of precipitation water was vertical at the initial stage. Saturated area was developing and extending 50 min before the collapse. 20 min before the collapse, we can see the lateral flow of the underground water. 1 s before the collapse, the lateral flow is significant at the lower part of the upper slope. From Fig. 20.10(b), it is almost uniform at the beginning of experiment. The saturated area seems to be charged in negative. The most interest point is the appearance of a large electric field around the slip surface area a few tens minutes before the collapse.

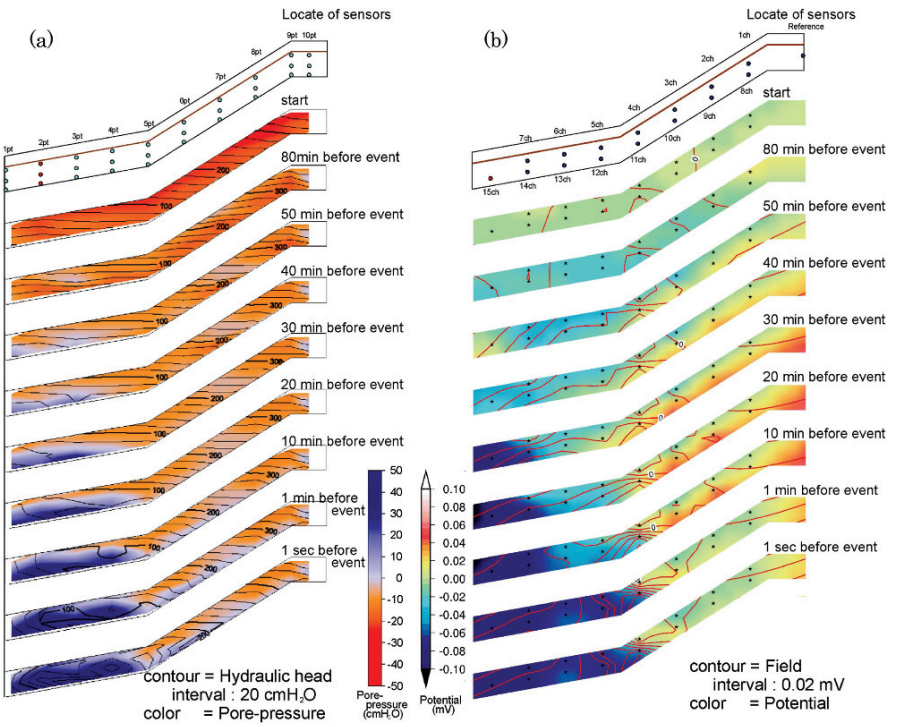

Fig. 20.10 2 dimensional maps of pore pressure and self-potential with time. (**a**) pore pressure and (**b**) electrical potential difference

A typical example of observed hydraulic and self-potential data is shown in Fig. 20.11. The position of the corresponding sensor is described at the top panel in the Fig. 20.10(a) (2 pt.) and (b) (15 ch). The curve of potential shows an interesting behavior. When the wetting front arrives at the position of electrode, the potential indicates the local minimum. While the area of the electrode turns to be saturated, the value shows the local maximum and a dramatic decrease. Furthermore, 30 min before the main slide, transient signals cam be seen only in self-potential changes. There is a remarkable step-like change around 90 min and rectangular changes around 105 min. These changes observed only below the upper boundary of the slipped body. The detected electric field is almost uniform. For the variation of pore pressure, transient signals such as impulsive and step-like changes are not described. The soil displacement data shows that the dislocation of the soil become apparent a few tens minutes before the collapse, so that there is a possibility that these transient signals are associated with dislocation of the soil.

20.8.4 Conclusion

Indoor laboratory experiment with simultaneous measurement of hydraulic, geotechnical, and electromagnetic approaches has been performed to investigate the rain-fall induced landslide process. It is found that self-potential variation seems to show the good relationship between hydrodynamics and electromagnetics and geotechnology and elecromagnetics. It means that there is a possibility to monitor the underground water condition or establish an early warning system of landslides with use of self-potential method.

Further analysis and experiments in both laboratory and in-situ field will be required to evaluate the electric phenomena with the hydrological and geotechnical changes. Such as pore pressure and the water flow out and geotechnical parameters such as the soil displacement.

Acknowledgment This work was partly supported by the JSPS Grants-in-Aid for Scientific Research #19403002, Research Foundation for the Electrotechnology of Chubu (REFEC), Chubu Electric Power Co. Inc., and NiCT R&D promotion scheme funding international joint research.

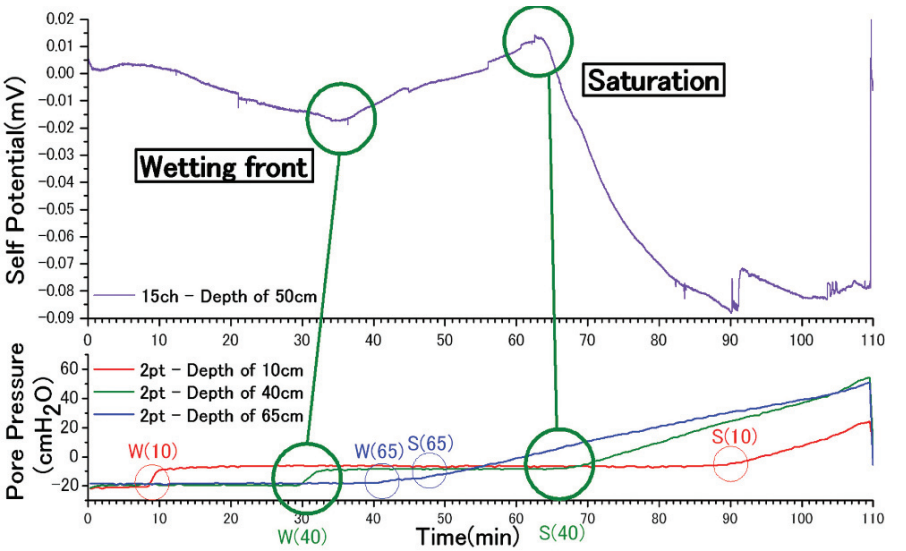

Fig. 20.11 A typical example of pore pressure and self-potential variation during artificial rainfall experiment. Time of the turning values of self-potential corresponds to the rise-times of pore pressure (wetting front and saturation)

20.9 A Real Time Debris Flow Warning System for the North Shore Mountains of Vancouver

Matthias Jakob, (BGC Engineering Inc., Canada)

Abstract The District of North Vancouver spans 160 km^2 at the foot of the North Shore Mountains that form the southernmost extension of the Coast Mountains. Numerous creeks draining the North Shore Mountains terminate as fans that have formed predominantly through debris flows. These fans have developed over the Holocene period, and those along the ocean inlets have become highly desirable properties due to low gradients, good drainage conditions and scenic locations. Between 1995 and 2003 a series of consultants reports have been released that quantified debris flow hazards and risk as well as propose engineering measures to reduce risk. Engineering measures on the highest priority creeks exceed the financial constraints of the District and thus a different risk reduction measure was chosen to compliment a long term risk reduction program in the form of a debris flow warning system. The Greater Vancouver Regional District has maintained records for some 15 years on the occurrence of landslides on the North Shore Mountains and some 32 storms were identified that had produced debris flows. An additional 32 storms that had not produced debris flows were selected based on rainfall amounts and intensity similar to those that had resulted in debris flows. A discriminant function analysis was conducted on all 64 storms for a large variety of rainfall antecedent and intensity variables to extract the significant discriminatory variables. The selected variables were the 4 week antecedent rainfall as well as the 2 day antecedent rainfall and the 48 h rainfall intensity. This function was able to correctly classify 80% of all cases. A high resolution calibrated weather forecast model designed and operated by the Geophysical Disaster Computational Fluid Dynamics Centre at the University of British Columbia is used to predict 48 h rainfall in one hour time steps, while the antecedent variables are calculated in real time for every approaching storm. The system is currently undergoing a testing phase and will be made operational in October of 2008.

20.9.1 Background

Debris flows are a common occurrence on the coastal mountains of British Columbia. They

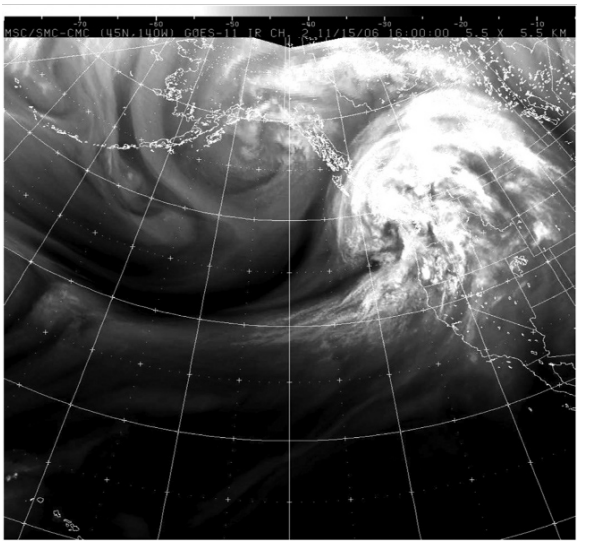

Fig. 20.12 Typical cyclone during late fall that can trigger debris flows along the North Shore Mountains (November 15, 2006)

occur primarily between October and January when numerous Pacific cyclones cross the coast with total rainfall amounts ranging between 40 and 150 mm and rainfall intensities up to 20 mm/h (Fig. 20.12). Debris flows are especially prevalent in areas logged over the past 15 years due to a pronounced loss in root strength and from poorly constructed logging roads. At the interface with urban development debris flows have impacted homes and other facilities. While the damages from debris flows on the North Shore Mountains pale in comparison with those in other countries, particularly the subtropical and tropical belts, the damage or potential damage affects a very affluent and increasingly risk adverse society. This fact has led to an active landslide risk management program with components of active engineering measures and warning systems.

20.9.2 Method

A large number of rainfall thresholds have been proposed for shallow landslides worldwide. These have recently been summarized by Guzzetti et al. (2008). Most are based on relations between rainfall intensity and duration and are plotted as envelopes below which shallow landsliding is unlikely and above which landsliding is possible. In the case of the North Shore Mountains, those thresholds are very low and application of an intensity-duration threshold for warning purposes would lead to tens of false warnings per year thus undermining the system's credibility (Fig. 20.13).

Previous work by Jakob and Weatherly (2003) has recognized that antecedent moisture conditions are crucial for explaining landslide occurrence and that the 4-week antecedent cumulative rainfall is the most significant variable in explaining the regional occurrence of shallow landsliding. Similarly to Jakob and Weatherly's study in 2003, antecedent and intensity data were gathered for all storms since 1990 that have caused shallow landslides in undisturbed (no logging or road building) terrain. An additional 32 storms were selected from the database over the same period with total rainfall amounts above 40 mm but for which no landslide records exist. Since the Greater Vancouver Regional District monitors the watersheds of the North Shore Mountains by helicopter after significant storms, it is believed that the assumption of no-landslides for those storms is reasonably correct. A forward stepwise discriminant function analysis was conducted on all 64 cases with the goal of (a) extracting the most significant variable to separate

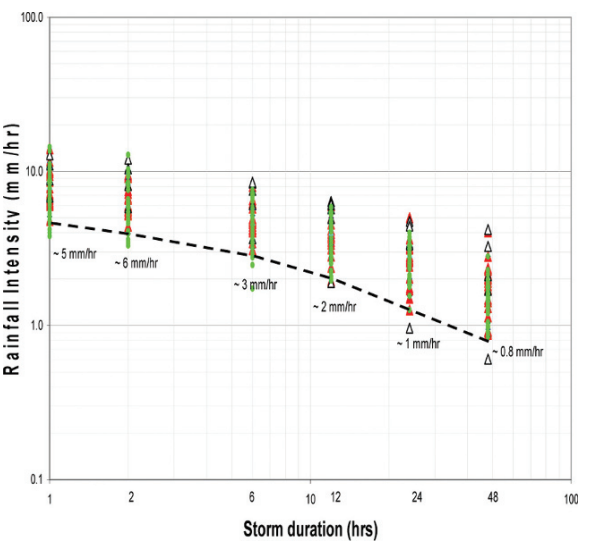

Fig. 20.13 Landslide Initiation Threshold for the North Shore Mountains

landslide from non-landslide initiating storms and (b) to create a discriminant function that allows calculation of the relative likelihood that a storm belongs to either group. The stepwise discriminant analysis identified three significant variables and the resulting function is shown in Eqs. (20.4) and (20.5).

$$\mathbf{LS} = -6.43 + 0.05A_{4\,W}; +0.28\mathrm{A}_{1\mathrm{d}} - 0.033\mathrm{A}_{5\mathrm{d}} \quad (20.4)$$

$$\mathbf{NLS} = -1.63 + 0.021A_{4\,W} + 0.104\mathrm{A}_{1\mathrm{d}} - 0.009\mathrm{A}_{5\mathrm{d}} \quad (20.5)$$

The results from the discriminant function analysis allow the real time calculation of a sliding time window of 4 week and 2 day antecedent rainfall based on rainfall records at the raingauge that was used for the original analysis. The 48-h rainfall intensity is being fed from a weather forecast model issued daily from the Geophysical Disaster Computational Fluid Dynamics Centre at the University of British Columbia. Using this statistic, a total of 75% of all landslide-triggering storms and 87.5% non-landslide triggering storms were correctly classified.

20.9.3 Debris Flow Warning Implementation

Section 20.3 summarized the development of a discriminant function model and classification functions for landslide and non-landslide initiating storms. Two of the variables (4 week and 2 day antecedent) will be measured via the DN25 rain gauge and be monitored real-time throughout the rainy season (between October 1 and April 30). The 48 h rainfall intensity will be produced from UBC's climate model.

Step 1: Backward computation of A_{4wk}, A_{2d}
Starting on October 1, every year, the four week and two day antecedent rainfall will be back-calculated from real-time data of the Berkeley rain gauge operated by BGC Engineering. The Berkeley gauge is not the calibration gauge, which is the DN25 gauge, but a regression analysis of monthly rainfall showed an almost perfect correlation ($r^2 = 0.99$) between the two gauges.

Step 2: Forward-looking prediction of the 48-h rainfall
Once a day, UBC's Geophysical Disaster Computational Fluid Dynamic Centre will forward their 48 h rainfall prediction for the North Shore Mountains. This data will arrive in the form of a meteogram, which will show the cumulative rainfall for pre-specified areas on the North Shore Mountains. At this point, predictions will be made for two rain gauge sites and forward looking calculations will be conducted simultaneously for these sites.

Step 3: Real-time calculation of the Classification Functions and ΔCS.
Both the A_{4wk}, A_{2d} variables and the Rainfall Intensity of 48-h will be entered into the classification functions. CS will be calculated as the difference between the LS and NSL function [$CS = F_{(LS)} - F_{(NLS)}$]. CS will then be plotted for the next 48 h. Implicit in these calculations is the recalculation of A_{4wk}, A_{2d} whenever a storm (as per definition in this report) is considered past. This re-calculation will occur on an hourly basis.

Step 4: Definition of Thresholds
The proposed real-time debris flow warning system will rely on the use of three separate thresholds, which are referred to as "Debris Flow Watch", and "Debris Flow Warning". These terms are defined as follows:

Debris Flow Watch
A debris flow watch will be issued when the CS line crosses negative one (-1) and more rainfall is being predicted in the next 48 h. The significance of a Watch is that hydroclimatic and hydrometeorological conditions are forming that provide conditions favourable for future debris flow occurrence. It is intended to provide information to those who need considerable lead time to prepare for a potential debris flow. It will include a qualitative statement of likelihood that the Advisory or Warning Levels will be exceeded. This qualitative statement will be: It is *likely* or *very likely* that the Warning Level will be reached. If it is unlikely that the

Warning level will be reached, no debris flow watch will be issued.

Debris Flow Warning
A debris flow Advisory will be issued with the CS line crosses the zero (0) line, and more rainfall is forecasted. In this instance, debris flow occurrence is *more likely than not* in the next 48 h and the predictions call for rainfall amounts in excess of 40 mm. This warning level is thus issued when hazardous weather conditions have developed, but the expected time of debris flow occurrence is still at least several hours in the future.

Step 5: Cancellation of Warning Levels
The cancellation of warning levels occurs in reverse order as described above. The debris flow warning is cancelled once the CS line drops below zero and forecasted rainfall for the next 48 h is below 40 mm. The debris flow watch is cancelled once the CS line drops below – 1 and forecasted rainfall for the next 48 h is below 40 mm.

20.9.4 Conclusions

This real time warning system will be the first regional operational debris flow warning system in Canada. It is expected that false warning will occur several times a year, which may eventually lead to some desensitizing of the population to warnings. However, for those individuals who live on creek fans created by debris flows, the debris flow watch and warning may provide sufficient time to leave their homes and stay in a safer place until the warnings have been cancelled. Over the long term, hazard avoidance or engineered mitigation measures are likely the preferred risk management option.

20.10 Study on Early Warning System for Debris Flow and Landslide in the Citarum River Basin, Indonesia

Kaoru Takara, Apip (Disaster Prevention Research Institute, Kyoto University, Japan), Agung Bagiawan (Water Resources Research Institute, Ministry of Public Works, Indonesia)

20.10.1 Introduction

This paper describes a distributed hydrological model of which advantage is to be able to calculate spatio-temporal patterns of rainfall-runoff and sediment transport dynamics in a catchment on a grid-cell basis. Since this model can quantitatively assess the possibility of the occurrence of debris flow and landslide in each grid-cell, it should be useful for early warning of sediment, debris flow and landslide disasters. The sediment runoff model are applied in the Lesti River which has small catchment located in the upper Brantas River basin, Indonesia as the case for study.

The objectives of this research are: (1) to verify the model performance by adding hillslope sediment transport algorithm and considering river channel routing processes to the model; (2) to illustrate how this model can be used for early warning; and (3) to develop a new method of lumping the distributed rainfall-runoff model to obtain a lumped-parameter model for larger river basins that require much computation time.

20.10.2 Physically-Based Distributed Model

The Cell Distributed Rainfall-Runoff Model Version 3 (CDRMV3) as a distributed hydrological model[1)] is used as a base of a distributed sediment transport model. The model includes a stage-discharge, *q*-*h*, relationship for both surface and subsurface flows[2)]:

$$q = \begin{cases} v_m d_m (h/d_m)^{\beta}, & 0 \le h \le d_m \\ v_m d_m + v_a (h - d_m), & d_m \le h \le d_a \\ v_m d_m + v_a (h - d_m) + \alpha (h - d_a)^m, & d_a \le h \\ v_m = k_m i, v_a = k_a i, k_m = k_a/\beta, & \\ \alpha = \sqrt{i}/n & \end{cases} \tag{20.6}$$

where q is discharge per unit width; h is water depth; i is the slope gradient; k_m is the saturated hydraulic conductivity of the capillary soil layer; k_a is the hydraulic conductivity of the non-capillary soil layer; d_m is the depth of the capillary soil layer; d_a is the depths of capillary and non-capillary soil layer; and n is the roughness coefficient based on the land cover classes. The continuity equation takes into account flow rate of each grid-cell or slope as:

$$\frac{\partial h}{\partial t} + \frac{\partial q}{\partial x} = r(t) \tag{20.7}$$

where t and x are time and distance along water flow, respectively; and r is the rainfall intensity.

The Lax-Wendroff finite difference scheme is used to solves the one-dimensional kinematic wave equation with the stage-discharge equation to simulate runoff generation and routing. The simulation area is divided into an orthogonal matrix of square grid-cells (250 m × 250 m).

20.10.3 Coupling of CDRMV3 and Sediment Transport Model

The concept of spatially distributed sediment runoff modeling is shown in Fig. 20.14. A sediment transport algorithm is newly added to the CDRMV3. Runoff generation, soil erosion and deposition are computed for each grid-cell and are routed between grid-cells following water flow direction. The sediment transport algorithm includes multiple sources of sediment transport, which are soil detachment by raindrop (DR) and hydraulic detachment or deposition driven by overland flow (DF). The basic assumption of this model is that the sediment is yielded when overland flow occurs. The eroded sediment is transported by overland flow to river channels.

Soil detachment and transport is handled with the continuity equation representing DR and DF as:

$$\frac{\partial (h_s c)}{\partial t} + \frac{\partial (q_s c)}{\partial x} = e(x,t) \qquad e(x,t) = DR + DF \tag{20.8}$$

where C is the sediment concentration in the overland flow (kg/m^3); h_s is the water depth of overland flow (m); q_s is the discharge of overland flow (m^3/s); and e is the net erosion (kg/m^2/h).

Soil detachment by raindrop is given by an empirical equation in which the rate is proportional to the kinetic energy of rainfall and decreases with increasing h_s. From the observation of rainfall characteristic in the study area[3] and dampening soil detachment rate by h_s[4], the empirical equation for DR for the ith grid-cell is expressed as:

$$DR_i = k\ KE e^{-b*h_{si}} = k\ 56.48\ r_i\ e^{-b*h_{si}} \tag{20.9}$$

where k is the soil detachability (kg/J); KE is the total kinetic energy of the net rainfall (J/m^2); and b is an exponent to be tuned.

Following the theoretical work of EUROSEM[4], the concept of transport capacity is used to determine sediment transport rates in overland flow.

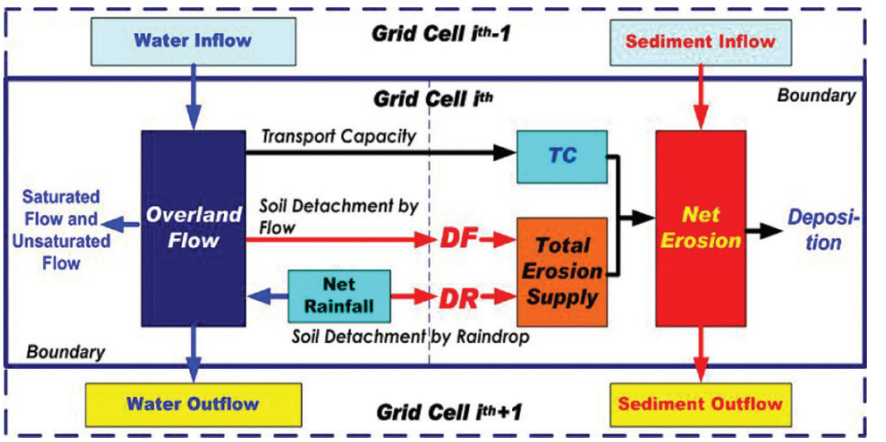

Fig. 20.14 Schematic diagram of the physically based rainfall-sediment-runoff model in the *ith* grid-cell scale

Sediment transport capacity of overland flow (TC) is defined as the maximum value of sediment concentration to transport, which is estimated for each grid-cell. Then for the *ith* grid-cell, DF is simulated as a result of overland flow and function of TC as follows:

$$DF_i = \alpha(TC_i/1000 - C_i)h_{si} \qquad (20.10)$$

where α is the detachment/deposition efficiency factor. Detachment or deposition by flow is assumed to be proportional to the TC deficit. Following the TC approach; if actual suspended sediment from upper grid-cells is lower than this capacity, detachment or erosion occurs, otherwise soil deposition excess.

The transportation capacity is calculated based on the Unit Stream Power (USP) theory. The USP theory contributing to TC is defined as a product of the overland flow velocity, v, and slope, i, in the *ith* grid-cell. A relationship between USP and the upper limit to the sediment concentration in the overland flow, C_t (ppm), can be derived[5] (see Eq. (20.11)). TC is the product of C_t as follows:

$$TC = \log C_t = I + J\log((vi - v_{critical}i)/\omega) \qquad (20.11)$$

in which:

$$I = 5.435 - 0.386\log(\omega D_{50}/NU) - 0.457\log(U^*/\omega)$$
$$J = 1.799 - 0.409\log(\omega D_{50}/NU) - 0.314\log(U^*/\omega)$$
$$\omega = \sqrt{\frac{2}{3} + \frac{36}{(\frac{\rho_s}{\rho_w} - 1)g(\frac{D_{50}}{1000})^{2/NU}}} - \sqrt{\frac{36}{(\frac{\rho_s}{\rho_w} - 1)g(\frac{D_{50}}{1000})^{2/NU}}} \qquad (20.12)$$

where vi is the unit stream power, m/s (v is flow velocity in m/s and i is the slope gradient m/m); $v_{critical}i$ is the critical unit stream power ($v_{critical}$ is the critical flow velocity); ω is the sediment fall velocity (m/s) calculated by Rubey's equation; ρ_s is the sediment particle density (kg/m^3); ρ_w is the water density (kg/m^3); g is the specific gravity (m/s^2); D_{50} is the median of grain size (mm); and NU is the kinematic viscosity of the water (m/s^2). $U^*(=\sqrt{gih_s})$ is the average shear velocity (m/s).

This model does not explicitly separate rill and interrill erosion. Gullying, river bed erosion, river bank erosion and lateral inflow of sediment to river channel are not considered.

20.10.4 Simulation Result

The model parameters to be determined are n (m$^{-1/3}$s), k_a (m/s), d_a (m), d_m (m), β, D_{50}(mm), k_s (kg/J), α, b, and $F1$ (ratio of rainfall lossed by interception or evapotranspiration processes). The regional sensitivity results show that six parameter $F1$, K_a, d_m, d_a, α, and k_s are sensitive and identified as compared to n, $beta$, D_{50}, and b.

One of the simulated flood events in calibration time is shown in Fig. 20.15. The predicted runoff and sediment concentration were compared with the observed one. The model is generally successful in representing broad trends in water discharge and sediment concentration, but water discharge tends to overestimated along times of rising limb and falling limb of hydrograph, the range of modeled sediment concentration is somewhat lower and higher than observed. A summary of this flood runoff event is given by the model efficiencies are: 0.854 (R^2: the coefficient of determination) and 0.251 ($RRMSE$). We may be able to recognize that the

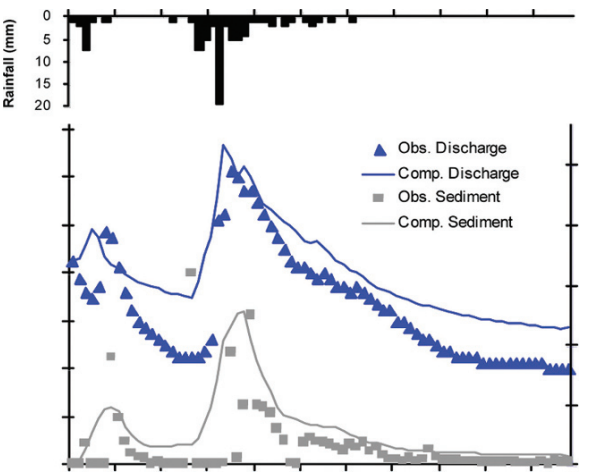

Fig. 20.15 Comparison of predicted sediment runoff with observed data for rainfall event 3–6 October, 2003

model prediction from an example is closer to the observed value.

An extensive sensitivity analysis utilized Monte Carlo simulation framework to produce an ensemble of sediment runoff simulation with respect to prescribed uncertainty in model parameters for each of the selected rainfall events was performed. To determine the uncertainty prediction at each time due to model parameters uncertainty, the predicted outputs were rangked to form a cumulative distribution function of the output variable based on the objective function selected, then the confidence intervals could be determined, which can be selected to represent the model uncertainty.

The calibrated model was applied to the discharge data sets for several rainfall events to test how well the calibrated parameters performed in reproducing an independent data set. These validation runs suggest that the hydrological condition is generally amenable to the hydrologically based on the distributed sediment runoff model under consideration.

20.10.5 Spatial Patterns of Erosion and Deposition

Figure 20.16 shows simulated erosion and deposition areas inside watershed for flood runoff event on 13–15 September 2004. A direct comparison with observed data is difficult since the threshold erosion rate above which these areas are mapped is not known. Figure 20.16 shows that the model was capable of locating the main sediment sources and sink within the Lesti River during this flood event. The model was also able to assign major erosion features. This three- dimensional representation shows that the simulated zones of soil detachment by flow are generally coupled with steep slopes and land use type, while the soil type assumed uniform over the catchment. Zones of deposition were simulated in valley bottoms and river banks.

The sediment transport algorithm for the distributed model includes multiple sources of sediment transport, which are soil detachment by raindrop and hydraulic detachment or deposition driven by overland flow. Estimations of the changes in total runoff and sediment yield with time and space in the catchment scale are required for solution of a number of problems. Design of dams and reservoirs, design of soil conservation, land-use planning, and water quality management are some of the examples. In addition, the processes controlling sediment runoff are complex and interactive. This complexity results in the term "erosion runoff processes" internal catchment area. The difficulty in the observation and measurement of the erosion and sediment transport processes during a runoff and erosion

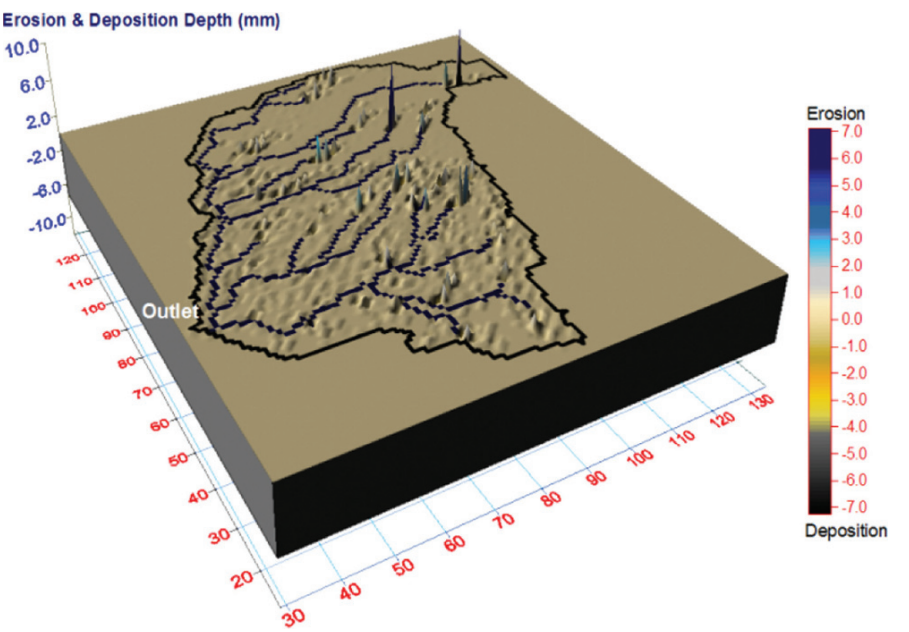

Fig. 20.16 Spatial distribution of erosion and deposition sources inside the catchment after rainfall event September 13–15, 2004

event due to small temporal and spatial scales makes necessary the use of a sediment runoff model for the spatio-temporal predictions of runoff, erosion, and deposition at the internal locations and catchment outlet. The recent developments of one dimensional model from this study are physically-based distributed sediment runoff model and its lumping which produced new lumped sediment runoff model version. Those models are used for the prediction of runoff and sediment transport processes at the catchment scale which facilitates the analysis of total sediment load in river channel and assists in the watershed and water resource management and planning. Application of this model to an Indonesian river basin is demonstrated.

20.11 Conclusion

As demonstrated here, the physically-based distributed rrainfall-runoff model can deal with overland flow, sediment yield, water content and some other elements relating to occurrence of debris flow and landslides at grid-cell scale on hillslopes. This has a potential ability for early warning of rainfall-induced sediment, debris flow and landslide disasters to be applied to small sized catchment, coupled with detail hydro-geo spatial information.

20.12 Other presentations

Development of a ubiquitous-based monitoring system for debris flows in Korea
Byung-Gon Chae (Korea Institute of Geoscience and Mineral Resources:KIGAM)

Development of Community-based Landslide Early Warning System in Indonesia
Dwikorita Karnawati (Department of Geological Engineering, Gadjah Mada University, Indonesia)

Distributed optical fiber sensors for precocious alerting of rainfall-induced flowslides
Luigi Zeni (Dept of Information Engineering, Second University of Naples)

Landslide geotechnical monitoring and mitigation measures in chosen location inside the SOPO Landslide Counteraction Framework Project, the Carpathian Mountains, Poland
Zbigniew Bednarczyk (Opencast Mining Institute, the Poltegor-Institute, Poland)

Preliminary Approach for a Nation-Wide Regional Landslide Early Warning System in South Korea
Dugkeun PARK*, Jeongrim OH*, Youngjin SON*, Minseok LEE (The National Emergency Management Agency (NEMA), Republic of Korea)

Rainfall height stochastic modelling as a support tool for landslides early warning
Roberto Greco (Seconda Università di Napoli, Italy)

Short-term weather forecasting for early warning
Pasquale Schiano, Paola Mercogliano, Gabriella Ceci (The Italian Aerospace Research Center (CIRA) and Euro-Mediterranean Centre for the Climate Change (C.M.C.C.)

Simple and low-cost wireless monitoring units for slope failure.
Taro Uchimura (University of Tokyo, Japan)

The warning criteria analysis of sediment runoff, debris flows, shallow landslides along the mountainous torrent
Tetsuya Kubota, Israel Cantu Silva, Hasnawir (Kyushu University)

References

Baum, R.L., Godt, J.W., Harp, E.L., McKenna, J.P. & McMullen, S.R. (2005). Early warning of landslides for rail traffic between Seattle and Everett, Washington, U.S. A. Proc. Int. Conf. on Landslide Risk Management, Vancouver, 731–740.

Baum, R.L., Savage, W.Z. & Godt, J.W. (2002). TRIGRS – a FORTRAN program for transient rainfall infiltration and grid-based regional slope stability analysis. US Geological Survey Open-File Report 02-0424.

Campbell, R.H. (1975). Soil slips, debris flows and rainstorms in the Santa Monica Mountains and vicinity, southern California. US Geological Survey Professional Paper 851.

Cascini L. & Versace, P. (1988). Relationship between rainfall and landslide in a gneissic cover. Proc. 5th Int Symp. on Landslides, Lausanne.

Chan, R.K.S., Pang, P.L.R. & Pun, W.K. (2003). Recent developments in the Landslip Warning System in Hong Kong. Proc. 14th Southeast Asian Geotechnical Conf.

Cole, K. & Davis, G.M. (2002). Landslide warning and emergency planning systems in West Dorset, England.

Instability: Planning and Management. London, Thomas Telford.
Damiano, E., Olivares, L., Minardo, A., Greco, R., Zeni, L., & Picarelli, L. (2008). Advanced monitoring criteria for precocious alerting of rainfall-induced flowslides. Proc. 10th Int. Symp. on Landslides, Xi'an, China, in press.
D'Orsi, R., d'Ávila, C., Ortigão, J.A.R., Dias, A., Moraes, L. & Santos, M.D. (1997). Rio-Watch: The Rio de Janeiro Landslide Watch System. Proc. 2nd Pan-American Symp. on Landslides, Rio de Janeiro, 1: 21–30.
Fathani, T.F. & Karnawati, D. (2007). Community-based early warning system at Central Java and East Java Province Indonesia, EWS Project – Final Report.
Finlay, P.G., Fell. R. & Maguire, P.K. (1997). The relationship between the probability of landslide occurrence and rainfall. Canadian Geotechnical Journal, 34: 811–824.
Flentje, P.N., Chowdhury, R.N., Tobin, P. & Brizga, V. (2005). Towards real-time landslide risk management in an urban area. Proc. Int. Conf. on Landslide Risk Management, Vancouver, 741–751.
Fukuoka, M. (1980) Landslides associated with rainfalls. Geotechnical Engineering, 11: 1–29.
Gasparini, P., Manfredi. G., & Zschau, J. (2007). Preface. Earthquake Early Warning Systems, Gasparini, P., Manfredi, G. & Zschau, J. eds., Springer, Berlin Heidelberg, V–XI.
Glade, T., Crozier, M. & Smith, P. (2000). Applying probability determination to refine landslide-triggering rainfall thresholds using an empirical Antecedent Daily Rainfall Model. Pure and Applied Geophysics, 157(6–8): 1059–1079.
Guzzetti, F., Peruccacci, S., Rossi, M. & Stark, C.P. (2008). The rainfall intensity-duration control of shallow landslides and debris flows: an update. Landslides 1(5): 3–18.
Hong, Y., Hiura, H., Shiona, K., Sassa, K., & Fukuoka, H. (2004). Quantitative assessment on the influence of heavy rainfall on the crystalline schist landslide by monitoring system – Case study on Zentoku landslide, Japan. Landslides 2(1): 31–41.
Ishido, T. & Mizutani, H. (1981). Experimental and theoretical basis of electrokinetic phenomena to rock-water systems and its applications to geophysics, Journal of Geophysical Research 86: 1763–1775.
Jakob, M. & Weatherly, H. (2003). A hydroclimatic threshold for landslide initiation on the North Shore Mountains of Vancouver, British Columbia. Geomorphology (54): 137–156.
Karnawati, D. & Fathani, T.F. (2008). Mechanism of earthquake induced landslides in Yogyakarta Province Indonesia, The Yogyakarta Earthquake, Star Publishing, California, 8-1–8-8.
Keefer, D.K., Wilson, R.C., Mark, R.K., Brabb, E.E., Brown, III W.M., Ellen, S.D., Harp, E.L., Wieczorek, G.F., Alger, C.S. & Zatkin, R.S. (1987). Real-time landslide warning during heavy rainfall. Science, 238: 921–926.
Lapenna, V., Lorenzo, P., Perrone, A., Piscitelli, S., Sdao, F. & Rizzo, E., (2005). Case history: 2D electrical resistivity imaging of some complex landslides in Lucanian Apennine (southern Italy), Geophysics, 70: B11–B18.
Mandolini, A. & Urciuoli, G. (1999). Previsione dell'evoluzione cinematica dei pendii mediante un procedimento di simulazione statistica. Rivista Italiana di Geotecnica, 33(1): 37–44.
Mills, K.A. (2002). Oregon's debris flow warning system. Geological Society of America Abstracts with Programs, 34(5).
Mitchue, M. (1985). A method for predicting slope failures on cliff and mountain due to heavy rain. Natural Disaster Science, 7(1): 1–12.
Ochiai, H., Okada, Y., Furuya, G., Okura, Y., Matsui, T., Sammori, T., Terajima, T. & Sassa, K. (2004). A fluidized landslid on a natural slope by artificial rainfall. Landslides, 3: 211–219.
Okada, K. (2004). Influence of rainfalls in prior to the earthquake. In: Sassa, K. Landslide disasters triggered by the 2004 Mid-Niigata Prefecture earthquake in Japan. Landslides 2(2): 135–142.
Perrone, A., Iannuzzi, A., Lapenna, V., Lorenzo, P., Piscitelli, S., Rizzo, E., & Sdao, F., (2004). High resolution electrical imaging of the Varco d7Izzo earthflow (southern Italy). **Journal** of **Applied Geophysics,** 56: 17–29.
Picarelli, L., Urciuoli, G. & Russo, C. (2004). The role of groundwater regime on behaviour of clayey slopes. Canadian Geotechnical Journal, 41: 467–484.
Picarelli, L., Versace, P., de Riso, R. & Palmieri, M. (2008). Landslide disaster management in Italy. Proc. 2007 Int. Forum on Landslide Disaster Management, Hong Kong, in press.
Picarelli, L., Versace, P., Olivares, L. & Damiano, E. (2007). Prediction of rainfall induced landslides in unsaturated granular soils for early waning setting up. Proc. 2007 Int. Forum on Landslide Disaster Management, Hong Kong.
Rizzo, E., Suski, B., & Revil, A., (2004). Self-potential signals associated with pumping tests experiments, Journal of Geophysical Research, 109: B10203, doi:10.1029/2004JB003049.
Rokhmana, C.A. (2007). The low cost monitoring system for landslide and volcano with digital photogrammetry, Proc. Joint Convention HAGI-IAGI-IATMI, Bali.
Saito, M. (1965). Forecasting the time of occurrence of slope failure. Proc. 6th Int. Conf. on Soil Mechanics and Foundation Engineering. Montreal, 2: 537–542.
Sasai, Y., (2008). Volcano-ElectroMagnetics in Japan: The 1986 Eruption of Izu-Oshima and the 2000 Caldera Formation of Miyake-jima Volcano, Electromagnetics in Seismic and Volcanic Area edited by Hattori and Telesca, Yubunsha Pub., 69–86.
Sassa, K., Fukuoka, H., Wang, G., Ishikawa, N. (2004). Undrained dynamic-loading ring-shear apparatus and application for landslide dynamics. Landslides 1(1): 7–19.
Senfaute, G., Merrien-Soukatchoff, V. & Morel, J. (2003). Microseismic monitoring applied to prediction of chalk cliffs collapses and contribution of numerical modelling. Proc. Int. Conf. on Fast Slope Movements. Prediction and Prevention for Rik Mitigation, L. Picarelli ed., Napoli, 1: 463–468.
Sirangelo, B. & Versace, P. (1992). Modelli stocastici di precipitazione e soglie pluviometriche di innesco dei movimenti franosi. Proc. XXIII Convegno Nazionale di Idraulica e Costruzioni Idrauliche, Florence, D361–D373.

Versace, P., Capparelli, G. & Picarelli, L. (2007). Landslide investigations and risk mitigation. The Sarno case. Proc. 2007 Int. Forum on Landslide Disaster Management, Hong Kong.

Versace, P., Sirangelo. B., & Capparelli, G. (2003). Forewarning model of landslides triggered by rainfall. Proc. 3rd Int. Conf. on Debris-Flow Hazards Mitigation: Mechanics, Prediction and Assessment, Davos.

Versace, P., Sirangelo, B. & Chirico, G.B. (1998). Analisi idrologica dell'innesco pluviometrico dell'evento di Sarno del 5 maggio 1998. C.N.R.-G.N.D.C.I., Publication n. 1925, Rome.

Wilson, R.C. & Wieczorek, G.F. (1995). Rainfall thresholds for the initiation of debris flows at La Honda, California. Environmental and Engineering Geoscience, 1(1): 11–27.

Zlotnicki, J. & Nisida, Y. (2003). Review of morphological insights of self-potential anomalies on volcano, Surveys in Geophysics., 24: 291–338.